

THE PHASE TRANSITION IN CHIRAL FLUID DYNAMICS*

MARLENE NAHRGANG, MARCUS BLEICHER

Institut für Theoretische Physik
Max von Laue-Str. 1, 60459 Frankfurt am Main, Germany

(Received October 2, 2009)

We present a chiral fluid dynamic model that allows for the dynamic study of the QCD phase transition and of the critical point. The non-equilibrium propagation of the chiral fields influences the fluid dynamic evolution of the quark fluid. This leads to inhomogeneities of the energy density in a discontinuous phase transition. When passing through a critical point the correlation length grows. This could be the basis for signatures of the critical point in heavy ion collisions.

PACS numbers: 25.75.Gz, 25.75.Nq

1. Introduction

One of the predominant features of the QCD phase diagram is the phase transition between the quark gluon plasma and the hadronic phase. It is well established by lattice QCD calculations that the phase transition at $\mu_B = 0$ is a crossover [1]. Model investigations [2] suggest that at low temperature but large μ_B the phase transition is discontinuous. As a consequence the line of this discontinuous phase transition must end in a critical point. Near criticality the thermodynamic quantities are governed by correlations that become long-range on the scale of the correlation length ξ .

The QCD phase diagram can partially be scanned in heavy ion collisions. By varying the beam energy different trajectories mapped to the $T-\mu$ plane can be studied. For trajectories passing through or near the critical point an increase of the fluctuations in observables should be visible [3, 4].

This work focusses on the explicit non-equilibrium propagation of the order parameter of chiral symmetry breaking coupled to an ideal fluid of quarks [6, 7]. The dynamics of this quark fluid is in return influenced by the phase transition.

* Presented at the International Meeting “Excited QCD”, Zakopane, Poland, February 8–14, 2009.

2. Chiral fluid dynamics

The dynamics are governed by the linear sigma model [8] with quarks

$$\mathcal{L} = \bar{q} [i\gamma\partial_\mu - g(\sigma + i\gamma_5\tau\vec{\pi})] q + \frac{1}{2} (\partial_\mu\sigma)^2 + \frac{1}{2} (\partial_\mu\vec{\pi})^2 - U(\sigma, \vec{\pi}), \quad (1)$$

with the constituent quark field $q = (u, d)$, the coupling g between the quarks and the chiral fields $\phi = (\sigma, \vec{\pi})$ and the potential for the chiral fields

$$U(\sigma, \vec{\pi}) = \frac{\lambda^2}{4} (\sigma^2 + \vec{\pi}^2 - \nu^2)^2 - h_q\sigma - U_0. \quad (2)$$

The parameters are chosen such that chiral symmetry is spontaneously broken in the vacuum, where $\langle\sigma\rangle = f_\pi = 93$ MeV and $\langle\vec{\pi}\rangle = 0$. The explicit symmetry breaking term is $h_q\sigma = f_\pi m_\pi^2$ with $m_\pi = 138$ MeV. Thus $\nu^2 = f_\pi^2 - m_\pi^2/\lambda^2$. Choosing $\lambda^2 = 20$ yields a sigma mass $m_\sigma^2 = 2\lambda^2 f_\pi^2 + m_\pi^2 \approx 600$ MeV. In order to have zero potential energy in the ground state $U_0 = m_\pi^4/(4\lambda^2) - f_\pi^2 m_\pi^2$.

The quark degrees of freedom are treated as a heat bath in local thermal equilibrium and are integrated out by

$$\mathcal{Z} = \int \mathcal{D}\bar{q}\mathcal{D}q\mathcal{D}\sigma\mathcal{D}\vec{\pi} \exp \left[\int_0^{\frac{1}{T}} d(it) \right] \int_V d^3x \mathcal{L}. \quad (3)$$

In a mean-field approximation \mathcal{Z} can explicitly be calculated and the grand-canonical potential at $\mu_B = 0$ gives the effective potential for the chiral fields in presence of the quarks

$$V_{\text{eff}}(\phi, T) = -\frac{T}{V} \log \mathcal{Z} = -d_q T \int \frac{d^3p}{(2\pi)^3} \log(1 + e^{-\frac{E}{T}}) + U(\sigma, \vec{\pi}), \quad (4)$$

with the degeneracy factor $d_q = 24$ and the energy $E = \sqrt{p^2 + g^2\phi^2}$ of the quarks. The quark mass $m_q^2 = g^2\phi^2$ is generated dynamically by non-zero values of the chiral fields in the chirally broken phase. At $\mu_B = 0$ the phase transition can be tuned by the coupling g as depicted in Fig. 1. We explicitly allow for a non-equilibrium propagation of the chiral field. With the scalar and pseudoscalar densities

$$\rho_S = g d_q \sigma \int \frac{d^3p}{(2\pi)^3} \frac{1}{E} f_{\text{FD}}(p), \quad \vec{\rho}_{\text{PS}} = g d_q \vec{\pi} \int \frac{d^3p}{(2\pi)^3} \frac{1}{E} f_{\text{FD}}(p) \quad (5)$$

the classical equations of motion are

$$\partial_\mu \partial^\mu \sigma + \frac{\delta U(\phi)}{\delta \sigma} = -g \rho_S, \quad \partial_\mu \partial^\mu \vec{\pi} + \frac{\delta U(\phi)}{\delta \vec{\pi}} = -g \vec{\rho}_{\text{PS}}. \quad (6)$$

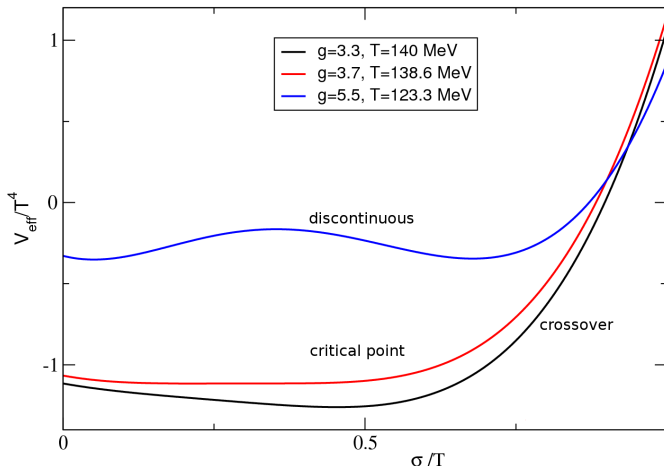


Fig. 1. V_{eff} at $\mu_B = 0$ for different couplings g and temperatures T to model the various strengths of the phase transition.

The evolution of the quark fluid is governed by local energy and momentum conservation. For an ideal fluid the energy-momentum tensor reads

$$T_{\text{fluid}}^{\mu\nu} = (e + p)u^\mu u^\nu - pg^{\mu\nu}, \quad (7)$$

where u^μ is the local four-velocity of the fluid and $g^{\mu\nu}$ the metric tensor. The local pressure and the local energy density are given by

$$p(\phi, T) = -V_{\text{eff}}(\phi, T) + U(\phi), \quad e(\phi, T) = T \frac{\partial p(\phi, T)}{\partial T} - p(\phi, T). \quad (8)$$

Locally, the chiral fields interact with the quark fluid and exchange energy and momentum. We thus have to include a source term

$$S^\nu = -\partial_\mu T_\phi^{\mu\nu} = g\rho_\sigma \partial^\nu \sigma + g\vec{\rho}_\pi \partial^\nu \pi, \quad (9)$$

where $T_\phi^{\mu\nu}$ is the energy-momentum tensor of the pure chiral field terms in (1). Within the fluid dynamic description of the quarks we have to solve

$$\partial_\mu \left(T_{\text{fluid}}^{\mu\nu} + T_\phi^{\mu\nu} \right) = 0. \quad (10)$$

3. Numerical results

The equations of motion for the chiral fields (6) are solved by a staggered leap-frog algorithm. For the solution of (10) we use the full 3 + 1d SHASTA fluid dynamic code [9–11].

3.1. Initial conditions

The equilibrium value of the sigma field σ_{eq} and the corresponding energy density e_{eq} (8) are calculated for an initial temperature $T_{\text{ini}} = 160$ MeV. The energy distribution is uniform in z -direction with $l_z = 6$ fm and ellipsoidal in the $x - y$ -plane

$$e(\vec{r}, t = 0) = \begin{cases} e_{\text{eq}} & \text{for } b^2x^2 + a^2y^2 < (ab)^2 \text{ and } |z| < l_z \\ 0 & \text{for } b^2x^2 + a^2y^2 > (ab)^2 \text{ or } |z| > l_z \end{cases} . \quad (11)$$

Here $a = r_A - \tilde{b}/2$ and $b = \sqrt{r_A^2 - \tilde{b}^2/4}$ where $\tilde{b} = 6$ fm is the supposed impact parameter and $r_A = 6.5$ fm the radius of the nuclei. The velocity profile is $v_z(\vec{r}, t = 0) = |z|/l_z \cdot v_{\text{max}}$, where $v_{\text{max}} = 0.2$. In the high energy region chiral symmetry is approximately restored, $\langle \sigma \rangle \approx 0$, and in the vacuum $\langle \sigma \rangle = f_\pi$. To have a smooth transition a Wood–Saxon distribution with is assumed

$$\sigma(\vec{r}, t = 0) = f_\pi + \frac{\sigma_{\text{eq}} - f_\pi}{(1 + \exp((\tilde{r} - \tilde{R})/\tilde{a}))(1 + \exp((|z| - l_z)/\tilde{a}))} + \delta\sigma(\vec{r}, t = 0) \quad (12)$$

with surface thickness $\tilde{a} = 0.3$ fm, $\tilde{r} = \sqrt{x^2 + y^2}$ and

$$\tilde{R} = \begin{cases} \frac{ab\tilde{r}}{\sqrt{b^2x^2 + a^2y^2}} & \text{for } \tilde{r} \neq 0 \\ a & \text{for } \tilde{r} = 0 \end{cases} . \quad (13)$$

The pion field is initially set to zero and neglected during the simulation. Initial fluctuations $\delta\sigma$ are put on top of (12). They are Gaussian distributed with a variance of 30 MeV and coarse grained in order to avoid an artificial correlation scale due to the grid spacing.

3.2. Time evolution

In Fig. 2 the energy density in the $x - y$ -plane at $z = 0$ is shown for four different times during the evolution through a critical point (left) and a discontinuous phase transition (right). Shortly after the expansion started both systems resemble each other. In the following the evolution of the systems is different. As expected for a discontinuous phase transition the expansion is slightly slower since the matter stays in the coexistence region for longer. Here we observe small patterns of high energy and of low energy clearly separated from each other. This indicates the nucleation and bubble formation due to the two degenerate minima. These inhomogeneities are non-equilibrium effects. For an evolution through the critical point this picture changes. The energy density is distributed more smoothly over the expansion volume.

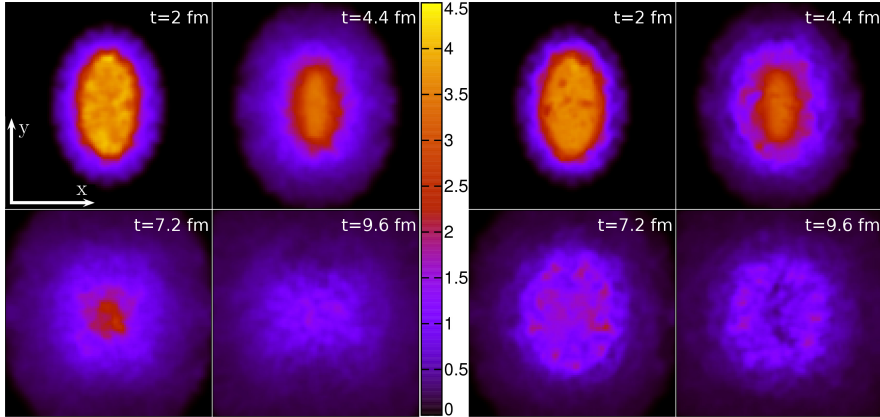


Fig. 2. Energy density in units of $e_0 = 148 \text{ MeV/fm}^3$ in the $x - y$ -plane at $z = 0$ for a continuous (left) and a discontinuous (right) phase transition.

3.3. Correlation length

Finite size effects limit the growth of the correlation length ξ in heavy ion collisions to about 6 fm [4]. Finite time effects are, however, more crucial. They prevent ξ from exceeding 2–3 fm [12, 13]. Even if at some early point of the collision the system above T_C was equilibrated it would be driven out of equilibrium passing through the critical point, a phenomenon known as critical slowing down. Since $1/\xi^2 = m_\sigma^2 = \delta^2 V_{\text{eff}}/\delta^2 \sigma|_{\sigma=\sigma_{\text{eq}}}$ the correlation length can be directly calculated in each cell. For an inhomogeneous medium different regions will cross the phase transition at different times. We consider all cells in a sphere with radius $r = 3 \text{ fm}$ in the hot and dense phase region around $\vec{r} = 0$. For small temperature intervals we average over the time of the expansion. Around the transition temperature T_C ξ grows but remains finite and stays within the limits of [12], see Fig. 3.

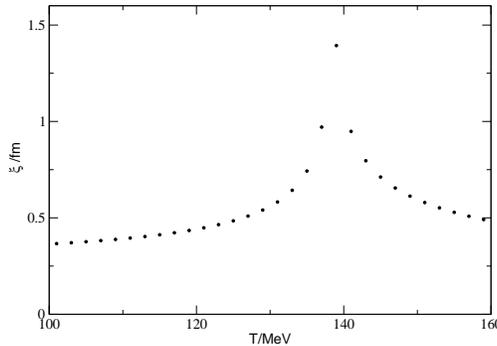


Fig. 3. ξ as a function of T for an evolution through a critical point. Due to critical slowing down ξ does not grow beyond approximately 1.5 fm at $T_C \simeq 139 \text{ MeV}$.

4. Conclusions

The most prominent effects of a non-equilibrium evolution through a phase transition were studied in the framework of chiral fluid dynamics. For a discontinuous phase transition bubble formation is seen and for a continuous phase transition the phenomena of critical slowing down is observed. The correlation length grows to roughly 1.5 fm.

The authors thank Adrian Dumitru for fruitful discussions. M.N. acknowledges financial support from the Polytechnische Gesellschaft Frankfurt am Main and the Helmholtz Graduate School of Heavy Ion Research.

REFERENCES

- [1] Z. Fodor, S.D. Katz, *J. High Energy Phys.* **04**, 050 (2004).
- [2] O. Scavenius, A. Mocsy, I.N. Mishustin, D.H. Rischke, *Phys. Rev.* **C64**, 045202 (2001).
- [3] M. Stephanov, K. Rajagopal, E.V. Shuryak, *Phys. Rev. Lett.* **81**, 4816 (1998).
- [4] M. Stephanov, K. Rajagopal, E.V. Shuryak, *Phys. Rev.* **D60**, 114028 (1999).
- [5] C. Nonaka, M. Asakawa, *Phys. Rev.* **C71**, 044904 (2005).
- [6] K. Paech, H. Stöcker, A. Dumitru, *Phys. Rev.* **C68**, 044907 (2003).
- [7] K. Paech, A. Dumitru, *Phys. Lett.* **B623**, 200 (2005).
- [8] M. Gell-Mann, M. Levy, *Nuovo Cim.* **16**, 705 (1960).
- [9] D.H. Rischke, S. Bernard, J.A. Maruhn, *Nucl. Phys.* **A595**, 346 (1995).
- [10] D.H. Rischke, Y. Pürsün, J.A. Maruhn, *Nucl. Phys.* **A595**, 383 (1995).
- [11] Y. Pürsün, diploma thesis, Goethe-Universität Frankfurt am Main (1993).
- [12] B. Berdnikov, K. Rajagopal, *Phys. Rev.* **D61**, 105017 (2000).
- [13] M. Asakawa, C. Nonaka, *Nucl. Phys.* **A774**, 753 (2006).